

Corridor Navigation of the Mobile Robot Using Image Based Control

Kyu Bum Han*

Graduated Student in Department of Mechanical Engineering, Yonsei University, Seoul 120-749, Korea

Hae Young Kim

Unitel Co., Ltd. Seoul 137-070, Korea

Yoon Su Baek

School of Electrical & Mechanical Engineering, Yonsei University, Seoul 120-749, Korea

In this paper, the wall following navigation algorithm of the mobile robot using a mono vision system is described. The key points of the mobile robot navigation system are effective acquisition of the environmental information and fast recognition of the robot position. Also, from this information, the mobile robot should be appropriately controlled to follow a desired path. For the recognition of the relative position and orientation of the robot to the wall, the features of the corridor structure are extracted using the mono vision system, then the relative position, the offset distance and steering angle of the robot from the wall, is derived for a simple corridor geometry. For the alleviation of the computation burden of the image processing, the Kalman filter is used to reduce search region in the image space for line detection. Next, the robot is controlled by this information to follow the desired path. The wall following control scheme by the PD control scheme is composed of two control parts, the approaching control and the orientation control, and each control is performed by steering and forward-driving motion of the robot. To verify the effectiveness of the proposed algorithm, the real time navigation experiments are performed. Through the result of the experiments, the effectiveness and flexibility of the suggested algorithm are verified in comparison with a pure encoder-guided mobile robot navigation system.

Key Words : Image Based Control, Mobile Robot, Wall Following Navigation, Kalman Filter, Hough Transform, Mono Vision System

1. Introduction

Autonomous mobile robot is defined as an automotive system which can move without human operation and can do various useful works. These systems can be seen more often in various real world applications such as transportation, cleaning, and surveillance tasks(Zheng, 1993). In

recent years, the study on the autonomous mobile robot system has become very active research area because of the following reasons:

1) The autonomous mobile robot has more possibility from the view of mobility and manipulability as compared with the fixed manipulator in the areas of industry or various service fields.

2) The remarkable development of computer and sensor technology promotes the development of the new type useful mobile robots.

The basic considerations in the study of the mobile robot systems are the efficient acquisition of the environmental information, namely environment modeling problem, and the fast recogni-

* Corresponding Author,

E-mail : satie90@hanmail.net

TEL : +82-2-2123-2827; FAX : +82-2-362-2736

Graduated Student in Department. of Mechanical Engineering Yonsei University, Seoul 120-749, Korea.

(Manuscript Received November 24, 2000; Revised May 11, 2001)

tion of the robot position during the navigation, namely localization problem.

For the solution of these problems, various sensors such as sonar(Kang and Lim, 1999), ultrasonic sensor, laser beacon, CCD camera have been tried out. Of these sensors, CCD camera has been more remarkable because it can offer fluent information in spite of the difficulty in real time applications. For the real time applications, many algorithms have been devised and proposed to overcome hardware limitations in many ways. And these algorithms have focused on reducing process time consumption as well as effective acquisition of the environmental information (Ayache, 1995).

The most important information in navigation task is the understanding of the 3-D structural information of the navigation environment. Several researches are as follows:

William(1989) studied real time navigation system of the mobile robot using "Structure from Motion" method. This method estimates the 3D structural information using two images acquired at different position by mono vision. From the consecutive two images, the vertical lines are extracted and matched by real time. For the successful application of this method, the accurate positions of the robot and camera are indispensable, so it can not be applicable in the systems where estimation performance is not satisfactory. Kröse and Groen (1997) computed the distance from the wall and robot orientation through the temporal derivatives of the optical flows using mono vision system. But the computation of the optical flow is very noise prone and computation load is very large. Kriegman et al., (1988) and Matthies and Shafer (1987) studied navigation system using stereo vision. They acquired two images of an environment and used to make path plan. But in this case, image process time is so large because of the stereo matching problem.

In this paper, we proposed a simple position estimation method to acquire relative position and the orientation of the mobile robot using mono vision system. Specially, for the real time application, the navigation environment is con-

strained to corridor structure and feature points in the mono image plane are extracted through geometrical property of the corridor structure. Also, for alleviation of the computation load, Kalman filter technique is used for line detection process. From the suggested algorithm, the robot position, off set distance from the wall and robot steering angle, can be efficiently computed and used to the mobile robot navigation control.

This paper is organized as follows: Section 2 presents the method of feature extraction in the image and computation of relative position of the mobile robot. Navigation control algorithm using PD control scheme is described in Sec. 3. In Sec. 4, the experimental equipment is briefly introduced and in Sec. 5, the experimental results on the real time wall following navigation using the suggested algorithm are given. Finally, in Sec. 6, conclusion and further studies are briefly remarked.

2. The Estimation of the Relative Position of the Robot

In the mono vision systems, the estimation of depth information of the environmental points is generally impossible because of the property of the perspective projection. Therefore, stereo vision system is used(Kriegman et al., 1988; Matthies and Shafer, 1987;Wallner et al., 1995; Jain et al., 1987) or two images are acquired from the two different position(William, 1989;Fennema et al., 1990;Takeshi, 1992;Straforini et al., 1992) for estimation of depth information. In stereo image systems, the matching algorithm of the two images is indispensable and the computation burden is increased. To avoid these defects, we estimate relative position of the mobile robot from the mono vision using the simple geometrical property of the corridor structure. Firstly, the features are defined as crossing points of horizontal lines of the floor and vertical lines of the doors. Next, the relative distance from the wall and orientation of the robot are computed using features and corridor geometry.

From this method, the relative position of the robot can be effectively estimated and com-

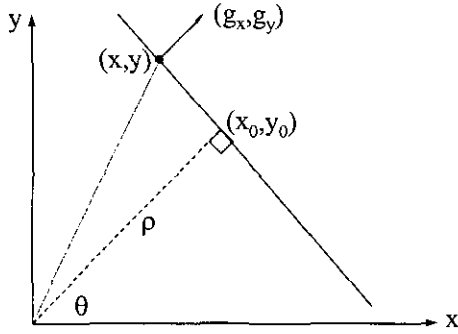


Fig. 1 Parameterization of a straight line

putational burden is decreased as well as navigation speed of the robot can be increased.

2.1 The line extraction in the corridor image

In order to extract the feature points, the line components in the image must be extracted previously. The widely used method for detection of geometrical factors in the image is Hough transform technique (Jain et al., 1995; Davies, 1997; Horn, 1987). Line detection procedure using Hough transform technique is as follows: The line component composed of detected edge points in the image can be transformed to the parameter space (ρ - θ space). Next, dominant parameters ρ and θ are selected using appropriately preset threshold value. Finally, the line component is detected by inverse Hough transform. Figure. 1 shows the parameterization of the line components.

The relationship between local pixel coordinate (x, y) and the corresponding local component of intensity gradient (g_x, g_y) for each edge pixel is as follows:

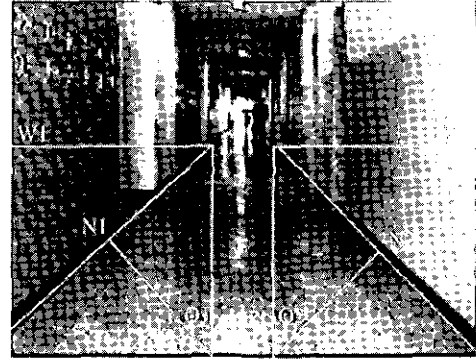
$$\frac{g_y}{g_x} = \frac{y_0}{x_0} \quad (1)$$

where (x_0, y_0) is taken as foot of the normal from the origin to the relevant line. Also, by the geometrical relationship

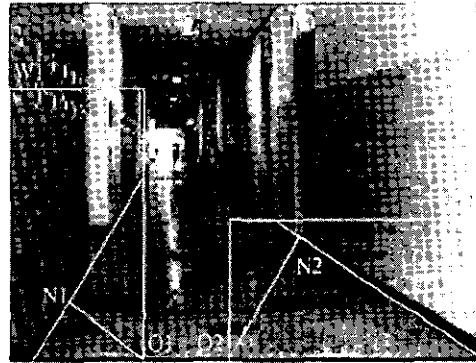
$$(x - x_0)x_0 + (y - y_0)y_0 = 0 \quad (2)$$

Using Eqs. (1) and (2), the unique foot of the normal can be computed as follows:

$$\begin{aligned} x_0 &= v g_x \\ y_0 &= v g_y \end{aligned} \quad (3)$$



(a) Initial search window



(b) Reset search window

Fig. 2 Search window setup

where

$$v = \frac{x g_x + y g_y}{g_x^2 + g_y^2}$$

Therefore the distance and orientation of the line from the origin can be given as

$$\rho = \frac{x g_x + y g_y}{(g_x^2 + g_y^2)^{1/2}} \quad (4)$$

$$\theta = \arctan(y_0/x_0) \quad (5)$$

All of the edge points are voted to the parameter space and most frequently occurred parameters are selected using the preset threshold value.

2.2 Kalman filter estimation in parameter space

In the application of the Hough transform, the defect is that it costs large computation time because whole image space should be searched. Also, line detection can be disturbed by noise. In order to reduce the searching time and for the

robustness to noise, we used Kalman filter estimation. The main purpose of Kalman filter in this study is to set up search window in image plane from the estimation of line parameters. Figure 2 shows the process of search windows setup.

The windows in Fig. 2(a) is initial search windows. Each x coordinate of W1 and W2 is always set as 0 and xsize and each y coordinates is varied to maintain the area of windows. Also, each y coordinate of O1 and O2 is always set as 0 and each x coordinate is determined by estimated values as follows:

$$X = \frac{90 - \theta}{90} \times \text{xsize}(\theta: \text{degree})$$

N1 and N2 is foot-of-normal points and the parameters (ρ, θ) are determined by O and N. If the parameters are predicted by Kalman filter, the search windows are reset up. Figure 2(b) shows the reset windows. X coordinates of O1 and O2 are changed by predicted parameters and the area of search windows are maintained. By the variation of search windows by Kalman filter, the image process space can be reduced and prevent the system from losing the line component.

The assumption is that the parameters that will be selected at next time step do not change abruptly from current selected parameters in parameter space. By this method, the search area in the parameter space can be reduced and search speed can be increased. Also because Kalman filter has ability of low pass filtering, the noise effect inherently contained in CCD camera can be somewhat removed.

The Kalman filter is defined as observer for the linear discrete stochastic system. It has simple filter structure and good convergence and ability to remove high frequency noise (low-pass filter).

The dynamic system is given by:

$$x(\kappa + 1) = Fx(\kappa) + v(\kappa) \quad (6)$$

$$x(\kappa) = \begin{bmatrix} \rho(\kappa) \\ \theta(\kappa) \\ \dot{\rho}(\kappa) \\ \dot{\theta}(\kappa) \end{bmatrix} \quad \text{and} \quad F = \begin{bmatrix} 1 & 0 & \Delta T & 0 \\ 0 & 1 & 0 & \Delta T \\ 0 & 0 & 1 & 0 \\ 0 & 0 & 0 & 1 \end{bmatrix}$$

where $v(\kappa)$ is a disturbance noise, Gaussian, zero-mean, temporally uncorrelated noise vector with

covariance Q, and T is sampling time.

Also, the measurement equation is given by:

$$y(\kappa) = Cx(\kappa) + \omega(\kappa) \quad (7)$$

$$y(\kappa) = \begin{bmatrix} \rho(\kappa) \\ \theta(\kappa) \end{bmatrix} \quad \text{and} \quad C = \begin{bmatrix} 1 & 0 & 0 & 0 \\ 0 & 1 & 0 & 0 \end{bmatrix}$$

where $\omega(\kappa)$ is measurement noise—a Gaussian zero-mean, temporally uncorrelated noise vector with covariance R.

In Kalman filter structure, the current state at time κ is predicted by the past state at time $\kappa-1$ and dynamic model on the assumption of constant target velocity as follows:

PREDICTION

$$\hat{x}(\kappa/\kappa-1) = F\hat{x}(\kappa-1/\kappa-1)$$

$$P(\kappa/\kappa-1) = FP(\kappa/\kappa)F^T + Q$$

where, $\hat{x}(\kappa/\kappa-1)$ is the time-updated state at time κ and $P(\kappa/\kappa-1)$ is the time-update covariance matrix. As P is increased, the uncertainty of the state is larger. After time-update prediction, the state and covariance matrix are updated by the measurement and time-updated data as follows:

FILTERING

$$K(\kappa) = P(\kappa/\kappa-1)C^T[CP(\kappa/\kappa-1)C^T + R]^{-1}$$

$$P(\kappa/\kappa) = [I - K(\kappa)C]P(\kappa/\kappa-1)$$

$$\hat{x}(\kappa/\kappa) = \hat{x}(\kappa/\kappa-1) + K(\kappa)[y(\kappa) - C\hat{x}(\kappa/\kappa-1)]$$

where, $K(\kappa)$ is Kalman gain at time κ . The initial state and covariance matrix is $\hat{x}(0/-1)$ and $P(0/-1)$. The initial parameters can be determined by Hough transformation in initial search windows.

2.3 Estimation of the position and orientation of the mobile robot from the wall

For navigation along specified path, it is needed to get information on offset distance from the wall and robot steering angle. Once the offset distance and steering angle are computed, these information can be used as feedback components for navigation control. Figure 3 shows the geometry for computing offset distance and steering angle of the robot to the wall. From the Fig. 3, the offset distance d and steering angle η can be simply computed. Let P_1 and P_2 be the points on the corridor line. The x coordinates of P_1 and P_2 are x_1 and x_2 . And in the same manner, z

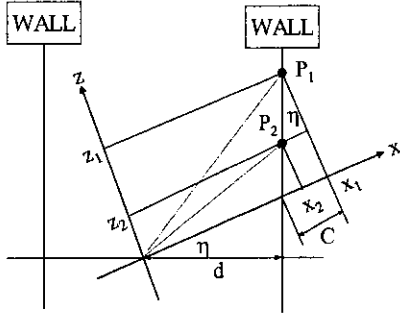


Fig. 3 Offset distance and steering angle

coordinates of P_1 and P_2 are z_1 and z_2 . From the camera perspective geometry, it gives

$$Y_1 = f_y \frac{y_1}{z_1} \quad (8)$$

where Y_1 is image plane coordinate and y_1, z_1 are camera coordinate.

Also, f_y is defined like Eq. (9) and can be acquired by camera calibration.

$$f_y = a_y f \quad (9)$$

where a_y is conversion factor between camera pixel and physical dimension and f is focal length. Because P is on the navigation floor, y component of the camera coordinate is given as

$$y = -\tan \varphi z + \frac{h}{\cos \varphi} \quad (10)$$

where φ is the tilt angle between camera optical axis and navigation floor and h is the height of the camera origin from the floor. So z_1 in Eq. (8) can be computed by Eqs. (8) and (10) as

$$z_1 = \frac{h f_y}{(Y_1 + f_y \tan \varphi) \cos \varphi} \quad (11)$$

Also, by the perspective geometry, it gives as

$$X_1 = f_x \frac{x_1}{z_1} \quad (12)$$

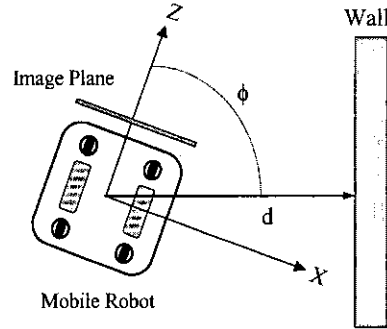
Similarly to Eq. (9), f_x is defined as

$$f_x = a_x f \quad (13)$$

where a_x is conversion factor between camera pixel and physical dimension. Thus x_1 is computed by Eqs. (11) and (12) as

$$x_1 = \frac{X_1 h f_y}{f_x (Y_1 + f_y \tan \varphi) \cos \varphi} \quad (14)$$

In the same manner, z_2 and x_2 is as follows



d : offset distance of the robot from the wall

ϕ : steering angle of the robot

v : translational velocity of the robot

$\dot{\phi}$: rotational velocity of the robot

Fig. 4 Top view of the mobile robot and corridor

$$z_2 = \frac{h f_y}{(Y_2 + f_y \tan \varphi) \cos \varphi} \quad (15)$$

$$x_2 = \frac{X_2 h f_y}{f_x (Y_2 + f_y \tan \varphi) \cos \varphi} \quad (16)$$

Next, the steering angle η is computed by the geometry of Fig. 3 as

$$\eta = \tan^{-1} \frac{x_2 - x_1}{z_2 - z_1} \quad (17)$$

To derive the offset distance d , C in Fig. 3 is derived as

$$C = z_1 \tan \eta \quad (18)$$

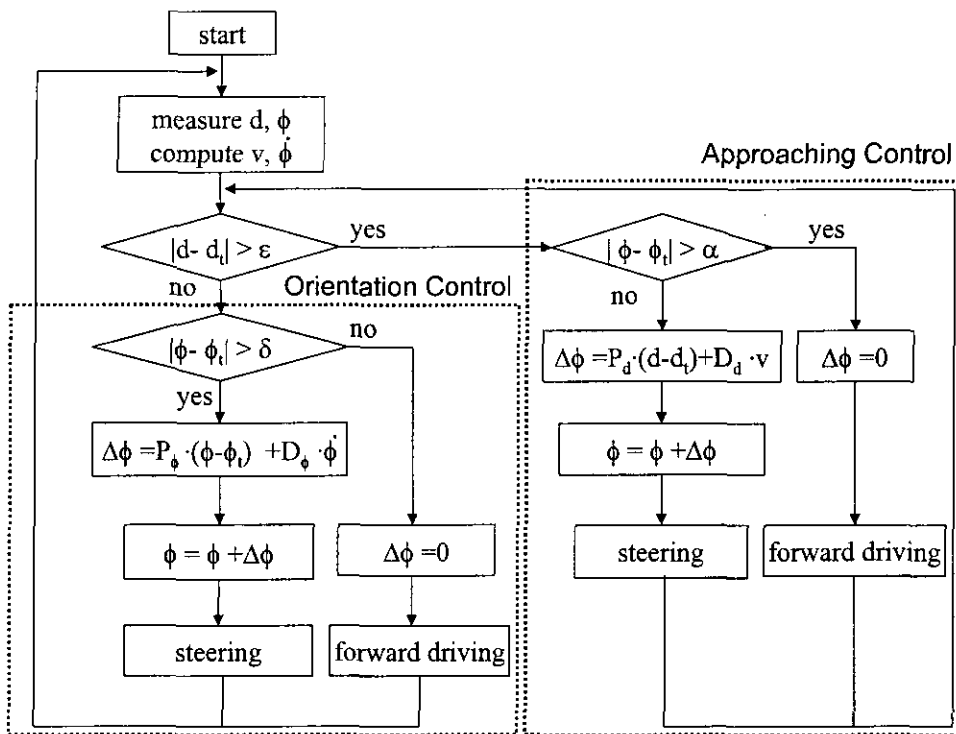
Finally, the offset distance d is computed as

$$d = (x_1 - C) \cos \eta \quad (19)$$

3. Navigation Control of the Mobile Robot Using PD Control Scheme

In this section, we explain the navigation control algorithm using the offset distance and steering angle derived in the previous section. The estimated offset distance from the wall (d) and steering angle ($\phi = 90 \pm \eta$) are used as feedback components so as to navigate the robot along specified path. Figure 4 shows the top view of the mobile robot and corridor.

In this study, the navigation object is to estimate the relative position of the robot and drive it maintaining the offset distance and steering angle of the robot to the target values d_t and ϕ_t . Figure 5 shows the flowchart of the navigation



d_t : target distance from the wall
 ϕ_t : target orientation of the robot
 α : maximum approach angle of the robot
 ϵ : minimum distance error
 δ : minimum progressing angle error

Fig. 5 Flowchart of the control algorithm

control algorithm.

In order to control the offset distance and steering angle of the robot simultaneously, the proposed navigation control algorithm is composed of the approaching control and orientation control. For each control, the basic motion of the robot is composed of steering and forward driving motion. After computation of the robot current position—the offset distance and orientation from the wall—and its derivatives, if the offset distance from the specified line is larger than preset minimum distance error, the robot approaches to the specified line(target distance from the wall). At this time, from the computation of the approach angle (the angle between corridor direction and mobile robot progressing direction, $\phi - \phi_t$), in case that the approach angle is deviated from the preset maximum approach angle α , the

robot moves straightly until the offset distance from the middle line of the corridor is smaller than ϵ . In case that the approach angle is smaller than the maximum approach angle α , the robot steers to approach the specified line.

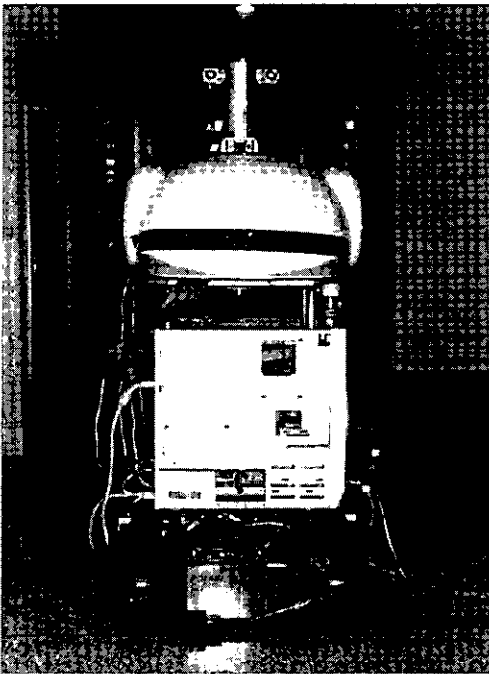
Once the robot is come to inside the maximum distance error ϵ , the navigation direction is controlled to the inside of minimum progressing angle δ . By using above sequential control algorithm, effective wall following navigation of the mobile robot can be achieved.

4. Experimental Equipment

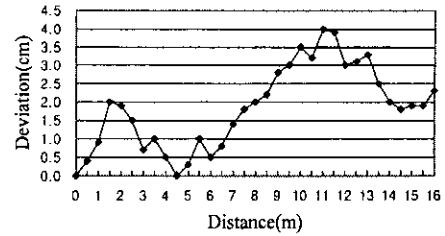
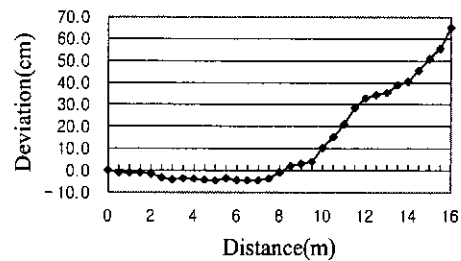
The experimental robot used in this study has six wheels—two driving wheels and four passive wheels. The driving wheels are driven independently. So it can change the direction at

Table 1 Specifications of the experimental robot

| Item | Specification |
|---------------------|--------------------------|
| Size | 700×700×1400 mm |
| Navigation velocity | 0-1000 mm/sec |
| Input voltage | 24V DC(12V 60AH battery) |
| Driving motor | DC servo motor |
| Encoder resolution | 0.0118 mm |

**Fig. 6** Appearance of the mobile robot

the current position and the trajectories of the forward driving and backward driving of the robot are same. Each driving wheels is controlled by DC motor and PWM type driver, and resolution of the attached encoder is 0.0118 mm/rev. For the navigation control, pentium 166 PC is took in the mobile robot and PCI bus type image acquisition board and motion control board for low level control are embarked. The rotation amount of the driving motor is computed through the inverse kinematics of the mobile robot. Figure 6 shows the appearance of the experimental mobile robot, and the specifications of the robot are shown in Table 1.

**Fig. 7** Wall following with encoder 1 (Pure navigation)**Fig. 8** Wall following with encoder 2 (External force added during navigation)

5. Experimental results

To verify the effectiveness of the suggested algorithm, real time wall following navigation is implemented. For the comparison with image based control, encoder based feedback control is performed previously. The encoder based feedback control purely relies on the encoder values of the two driving wheels and precise estimation of the robot position is nearly impossible. Total navigation distance is 16m and the navigation speed is 25cm/sec. Figure 7 shows the experimental result by encoder based feedback control.

Once error source is generated during the navigation, the robot is deviated from the specified path—the middle line of the corridor, and navigation fails as navigation distance is increased for the accumulation of the deviation. The error sources are discordance of two driving wheels, sliding effect between the wheels and floor and so on. These effects are more clearly observed in Figure 8. Fig. 8 shows the result of encoder based feedback control added external force during navigation.

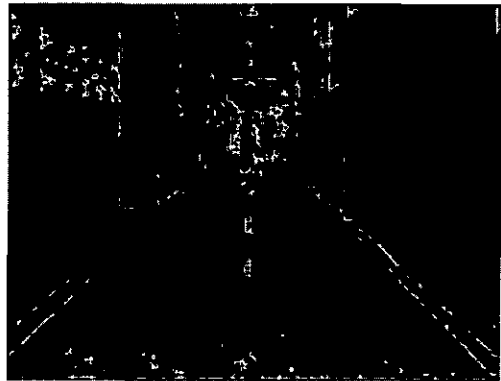
If the steering angle changes abruptly by

Table 2 Covariance matrices for Kalman filter

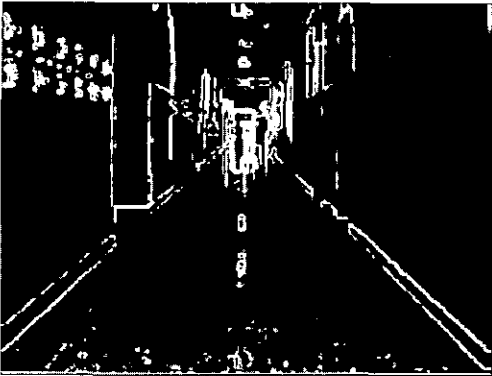
| Q | P | Size of search window |
|----------------------|----------------|---------------------------------|
| Diag{10, 20, 10, 20} | Diag{1.0, 1.0} | 20×5 (ρ - θ space) |



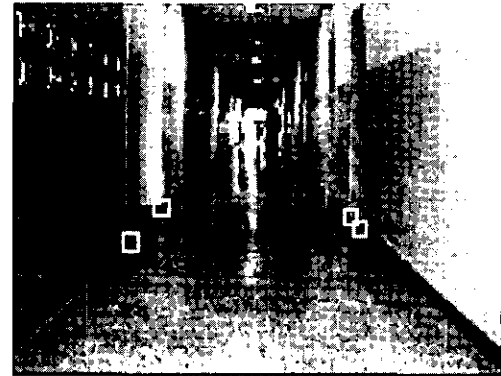
(a) View of the corridor



(b) Extraction of the edge



(c) Thinned edge image



(d) feature point extraction

Fig. 9 Corridor and feature points

external force during navigation, the robot should compensate the deviation and return to the previous direction. But the error source is generated and the navigation fails by accumulation of the errors. External force is added at 8m after navigation start and the deviation is increased as navigation distance is farther. For the solution of this defect of encoder based feed back, we used information by the CCD image as feed back component. The crossing points of the corridor line and vertical door line are selected as feature points, and the positions of feature points are detected by image processing. The lines are extracted by edge detection followed by Hough transform. Then the relative positions of features

are computed, and the offset distance from the wall and steering angle are computed by the method explained in Sec. 3.

Figure 9 shows the images. Figure 9(a) is the view of corridor, (b) is the extraction of the edge by the Sobel operator, (c) is the thinned edges from (b), finally, (d) is the extracted feature points.

Also, the covariance matrices for Kalman filter to detect line component in Sec. 2 are preset like Table 2. The elements of the matrices are determined by the trial and error method empirically.

Figure 10 shows the result of image based control by proposed navigation algorithm. Similarly to the encoder based feedback control,

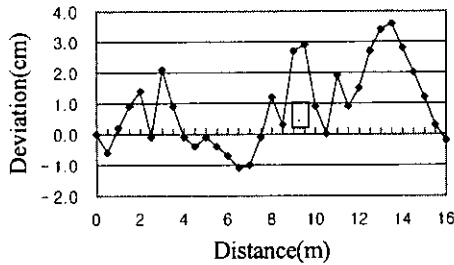


Fig. 10 Wall following with CCD camera 1 (Pure translation)

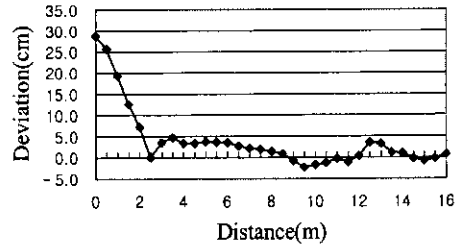


Fig. 12 Wall following with CCD camera 3 (Initially deviated)

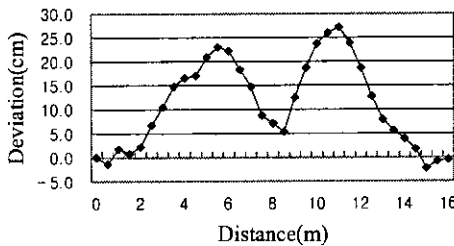


Fig. 11 Wall following with CCD camera 2 (External force added during navigation)

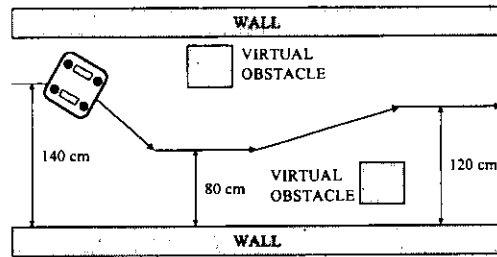


Fig. 13 Virtual obstacle avoidance navigation

the navigation distance is 16m and navigation speed is 25 cm/sec, and sampling period is 0.14 sec.

If the offset distance d is deviated from preset range, the deviation is compensated from the measured information by CCD camera. It is observed that the deviation of the robot is maintained less than 50 mm from the middle line of the corridor from Fig. 10. Also, in order to observe the effect of the external disturbance, we added external force to the robot during navigation. Figure 11 shows the result.

Similar to the encoder based feedback control, we let the steering angle change abruptly by external force at 5m and 8m from the navigation start, but the error was compensated at once by feature extraction in the image.

Finally, we let the robot be placed away from the middle line and have inclined to the corridor direction initially. The initial offset deviation is 30 cm from the middle line and the steering angle deviation is 3 degree. Figure 12 shows the result.

Initial offset deviation is gradually decreased and finally converged to the middle line of the corridor with error less than 50 mm. From the

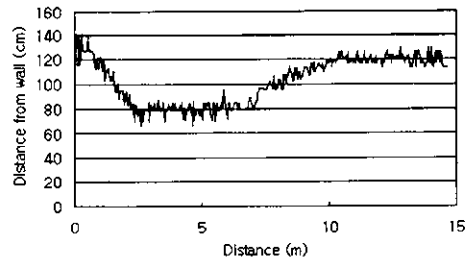


Fig. 14 Experimental result of virtual obstacle avoidance navigation

comparison with the encoder based feedback control, the image based navigation control by proposed algorithm is more effective and robust to the disturbance. Next, we assume virtual obstacles like Fig. 13, and control the robot to avoid the obstacles and follow the planned path.

The virtual obstacles are assumed as 20cm × 20cm rectangle box. To avoid the obstacle, the robot trajectory is planned as follows: Initially, the robot is at the 130 cm offset point from the middle line, and moves to the 80cm offset point, then to 120 cm offset point. Figure 14 shows the offset distance measured from the CCD camera.

Total navigation time is 72 sec and average speed is 25 cm/sec. From the result, we concluded that the robot could navigate the desired path

effectively using the offset information from the single CCD camera.

6. Conclusions

In this study, the navigation system of the mobile robot using mono vision is described and the performance of the proposed algorithm is verified by PC based real time wall following navigation. Specially, the feature points are extracted from mono CCD camera and the relative position of the robot is computed through the simple corridor geometry. Then the PD control algorithm using the information of relative position is suggested.

Also, for the time efficiency in image processing and robustness, the Kalman filtering is employed to predict the parameters of corridor line in parameter space and to set up search windows. By the application of the Kalman filter, we have reduced 25% of the line detection time in image processing in comparison with the full image region search.

In order to verify the effectiveness of the proposed algorithm, two types of image based navigation experiments are performed. The first experiment is for navigation along the middle line of the corridor, while the second one is virtual obstacle avoidance. For the comparison, we implemented encoder based feedback control. In the encoder based control, small error of the feedback can cause deviation of the trajectory, and thus the navigation has been failed. But in image based navigation, the robot has ability to cope with external disturbances. By simple modeling of the navigation environment and efficient image processing, fast navigation could be achieved. The average navigation speed of the mobile robot in our experiment is 25cm/sec, the total navigation distance is 16m and total sampling time is 0.14sec. Also, we implemented virtual obstacle avoidance navigation to show the following performance to the planned trajectory. Henceforth, more accurate and fast estimation technique as well as consideration on more complicated environment will be studied.

References

- Ayache, N., 1995, *Artificial Vision for Mobile Robot: Stereo Vision and Multi sensory Perception*, MIT Press.
- Davies, E. R., 1997, *Machine Vision*, Academic Press.
- Fennema, A. Hanson, E. Riseman, Beveridge, J. R. and Kumar, R., 1990, "Model-Directed Mobile Robot Navigation," *IEEE Trans. on System, Man and Cybernetic*, Vol. 20, no. No, pp. 1352~1369.
- Horn, K. P., 1987, *Robot Vision*, MIT Press.
- Jain, R., Bartlett, S. L. and O'Brien, N., 1987, "Motion Stereo Using Ego-Motion Complex Logarithm Mapping," *IEEE Trans. on Pattern Analysis and Machine Intelligent*, Vol. 9, No. 3, pp. 356~369.
- Jain, R., Kastury, R. and Schunck, B. G., 1995, *Machine Vision*, McGraw Hill.
- Kang, S. K. and Lim, J. H., 1999, "Sonar Based Position Estimation System for an Autonomous Mobile Robot Operating in an Unknown Environment," *KSME International Journal*, Vol. 13, No. 4, pp. 339~349.
- Kriegman, D. J., Triendl, E. and Binford, T. O., 1988, "Stereo Vision and Navigation in Buildings for Mobile Robots," *IEEE Trans. on Robotics and Automation*, Vol. RA-5, No. 6, pp. 45~65.
- Kröse, Dev B. and Groen, F., 1997, "Navigation of a Mobile Robot on the Temporal Development of the Optic Flow," *Proc. IEEE/RSJ Int. Conference on Intelligent Robot and Systems*, Vol. 2, pp. 558~562.
- Lewis, F. L., 1992, *Applied Optimal Control and Estimation*, Prentice Hall.
- Matthies, L. and Shafer, S. A., 1987, "Error Modeling in Stereo Navigation," *IEEE Trans. on Robotics and Automation*, Vol. RA-3, No. 3, pp. 239~248.
- Straforini, M. Coelho, M. C. Campani, M., and Torre, V. M., 1992, "The Recovery and Understanding of a Line Drawing from Indoor Scenes," *IEEE Trans. on Pattern Analysis and Machine Intelligent*, Vol. 14, No. 2, pp. 298~303.
- Takeshi, S., 1992, "3-D Corridor Scene

Modeling from a Single View Under Natural Lightning Conditions," *IEEE Trans. on Pattern Analysis and Machine Intelligent*, Vol. 14, No. 2, pp. 293~298.

Wallner, F., Graf, R. and Dillman, R., 1995, "Real-Time Map Refinement by Fusing Sonar and Active Stereo Vision," *IEEE Int. Conference*

on Robotics and Automation, pp. 2968~2973.

Willam, M., 1989, "Visual Estimation of 3-D Line Segment from Motion A Mobile Robot System," *IEEE Trans. on Robotics and Automation*, Vol. 5, No. 6, pp. 820~825.

Zheng, Y. F. 1993, *Recent Trends in Mobile Robots*, World Scientific.